

# Non-flammable fluorine-phosphorus-based polymer electrolytes for high-performance all-solid-state lithium metal batteries

Enchi Hu,<sup>a</sup> Songtao Li,<sup>a</sup> Guanyu Zhong,<sup>a</sup> Zhengtao Mai,<sup>a</sup> Siheng Zhang,<sup>a</sup> Jianda Niu,<sup>a</sup> Zhixian Dong,<sup>a</sup> Jinbao Xu,<sup>\*,a</sup> Zhan Wang,<sup>\*,b</sup> and Caihong Lei<sup>\*,a</sup>

## 1. Experiments

### 1.1 Materials

The chemical reagents used in the experiment were all commercially available analytical grade or battery-grade reagents and were used directly without further purification. Specific materials include: diethyl ether (purity  $\geq 99\%$ ), triethylamine (TEA, 99%), hydroxyethyl acrylate (HEA, 97%), phenylphosphoryl dichloride (PPD, 98%), 2,2,2-trifluoroethyl acrylate (TFEA, 99%), poly(ethylene glycol) methyl acrylate (PEGMA,  $M_n = 480 \text{ g}\cdot\text{mol}^{-1}$ , 99%), N-methyl-2-pyrrolidone (NMP, GC), polyvinylidene fluoride (PVDF,  $M_w = 400,000 \text{ g}\cdot\text{mol}^{-1}$ , 99%, Canrd), lithium bis(trifluoromethanesulfonyl) imide (LiTFSI, battery grade), azobis(isobutyronitrile) (AIBN, 99%), lithium iron phosphate (LiFePO<sub>4</sub>, LFP, Macklin, battery grade), and conductive carbon black Super P (Canrd, battery grade). Cellulose membrane (NKK TF4030) was employed as scaffolds. All materials were stored and used in an argon-filled glove box (Mikrouna, H<sub>2</sub>O and O<sub>2</sub> content  $< 0.01 \text{ ppm}$ ).

### 1.2 Characterizations

Proton nuclear magnetic resonance (<sup>1</sup>H NMR) spectra were conducted on a Bruker AV400 NMR spectrometer by using deuterated chloroform (CDCl<sub>3</sub>) as the solvent and tetramethylsilane (TMS) as the internal standard. Fourier-transform infrared (FT-IR) spectra were recorded on a FT-IR-Digilab FTS3100FTIR spectrometer with potassium bromide (KBr) pellet. The surface and cross-section morphologies of the films were observed by JEOL JSM-6700F scanning electron microscopy (SEM) after 60 seconds platinum sputtering. Thermogravimetric analysis (TGA) was performed on a TA SDT Q600 instrument under a nitrogen atmosphere at a heating rate of  $10 \text{ }^\circ\text{C min}^{-1}$  in the range of 25 to 800  $^\circ\text{C}$ . The crystallization behavior was investigated using differential scanning calorimetry (DSC) on a Mettler Toledo DSC3 machine with a sweep speed of  $10 \text{ }^\circ\text{C min}^{-1}$  and a measurement temperature range of  $-60 \text{ }^\circ\text{C}$  to  $150 \text{ }^\circ\text{C}$  in a nitrogen flow atmosphere. The X-ray photoelectron spectrometer (XPS, ESCA Lab 250 Xi) was employed to analyze the electrode characteristics after electrochemical cycling.

The ionic conductivities of the new electrolytes were characterized by electrochemical impedance spectroscopy (EIS) on a VMP3B-10 electrochemical workstation at an AC amplitude of 10 mV with a frequency range from 1 MHz to 10 mHz. A stainless-steel sheet (SS) was used as the blocking electrode to carry out the EIS measurements and the ionic conductivity was calculated by equation (1):

$$\sigma = \frac{L}{R \times S} \quad (1)$$

where L, R, and S stand for the thickness of electrolytes, the impedance of the bulk electrolyte, and the contact area between the two stainless-steel sheets, respectively.

The lithium-ion transference number ( $t_{Li^+}$ ) was characterized by chronoamperometry (VMP3B-10 electrochemical workstation) and the  $t_{Li^+}$  was calculated on the basis of equation (2):

$$t_{Li^+} = \frac{I_s \times (\Delta V - I_0 \times R_0)}{I_0 \times (\Delta V - I_s \times R_s)} \quad (2)$$

where  $\Delta V$  is the potential difference (10 mV),  $I_0$  and  $I_s$  are the initial current and the steady-state current before and after polarization, respectively, while  $R_0$  and  $R_s$  are the interfacial resistances before and after polarization.

The electrochemical stability window (ESW) of the electrolyte was measured by using linear sweep voltammograms (LSV) in a voltage range of 2 to 6 V (vs. Li/Li<sup>+</sup>) at a scanning rate of  $1 \text{ mV s}^{-1}$  by using CR-2032 batteries of SS/TDP/Li.

The galvanostatic cycling measurement of Li/TDP/Li batteries was carried out on a CT-1008-S1 charge/discharge instrument (Neware) and all the batteries were cycled for 1 h of charge and the subsequent 1 h of discharge.

The cycling performance and rate capability of LFP/GPE/Li batteries (CR2032) were conducted on a battery test system (CT-1008-S1, Neware) under different potential ranging from 2.5 to 4.0 V at room temperature.

### 1.3. Synthesis of DABP

Under an ice bath, HEA (34.80 g, 0.30 mol) and TEA (30.30 g, 0.30 mol) were dissolved in 100 mL of anhydrous ether and transferred to a thoroughly dried 250 mL round-bottom flask. At  $0 \text{ }^\circ\text{C}$ , PPD (29.30 g, 0.15 mol) dissolved in 20 mL ether was slowly added to the reaction mixture *via* a constant pressure dropping funnel, with the addition lasting approximately 1 h. The reaction was exothermic and accompanied by the evolution of white gas, so the addition rate was controlled. After completing the dropwise addition, the ice bath was removed, and the mixture was stirred at room temperature for another 12 h to complete the reaction. The reaction mixture was filtered to remove the byproduct triethylamine hydrochloride. The organic phase was washed three times with  $1 \text{ mol}\cdot\text{L}^{-1}$  hydrochloric acid solution, 10% sodium bicarbonate solution, and saturated sodium chloride solution. The organic phase was dried over anhydrous sodium sulfate, and the solvent was

removed under vacuum at 30 °C to obtain a colorless oily product DABP with a yield of 73.6% (39.1 g). The structure was confirmed by  $^1\text{H}$  NMR and FT-IR (Fig. S2). FT-IR:  $1250\text{ cm}^{-1}$  (P=O),  $1438\text{ cm}^{-1}$  (P-Ph),  $1725\text{ cm}^{-1}$  (C=O) and  $1635, 1410, 812\text{ cm}^{-1}$  (C=C).  $^1\text{H}$  NMR (400MHz,  $\text{CDCl}_3$ , ppm,  $\delta$ ): 7-8 (10H, aromatic), 6.4 (1 H,  $\text{CH}_2=$ , trans to H), 6.1 (1H,  $-\text{CH}=\text{}$ ), 5.9 (1H,  $\text{CH}_2=$ , cis to H), 4.1–4.3 (4H,  $-\text{CH}_2-\text{CH}_2-$ ).

#### 1.4 Synthesis of SPE

TDP118 was described as an example, where TFEA, DABP and PEGMA were in a molar ratio of 1:1:8. TFEA (0.11 g), DABP (0.22 g), PEGMA (2.67 g), and LiTFSI (0.60 g) were added into a glass bottle and stirred at room temperature until LiTFSI was completely dissolved. Afterward, AIBN (0.03 g) thermal initiator was added and stirred at room temperature. The resulting homogeneous solution was uniformly coated onto a cellulose membrane and placed in a PTFE mold, then heated at 80 °C for 3 h to complete the radical crosslinking polymerization.

#### 1.5 Preparation of LFP cathodes

The LFP cathode was prepared with a conventional casting method: LFP (0.80 g) active particles, super-P (0.10 g) and PVDF binder (0.10 g) were dispersed in NMP solvent, which was then uniformly coated on an aluminum foil by a scraper blade. After that, the cathode was kept at 60 °C under vacuum for 72 h to remove the residual solvent. The area specific density of the LFP was about  $2.50\text{ mg cm}^{-2}$ .

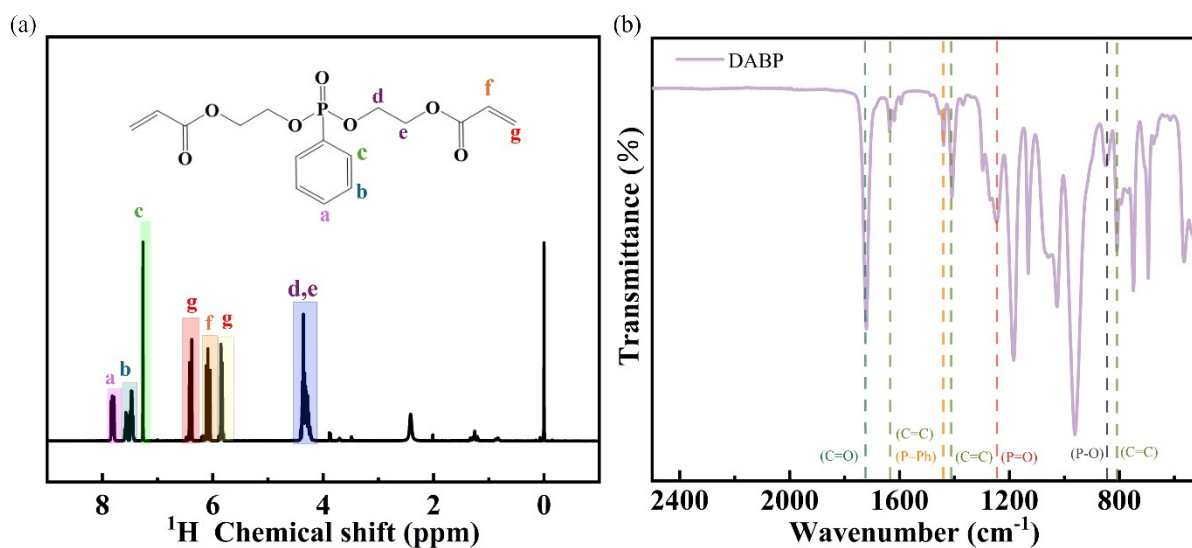
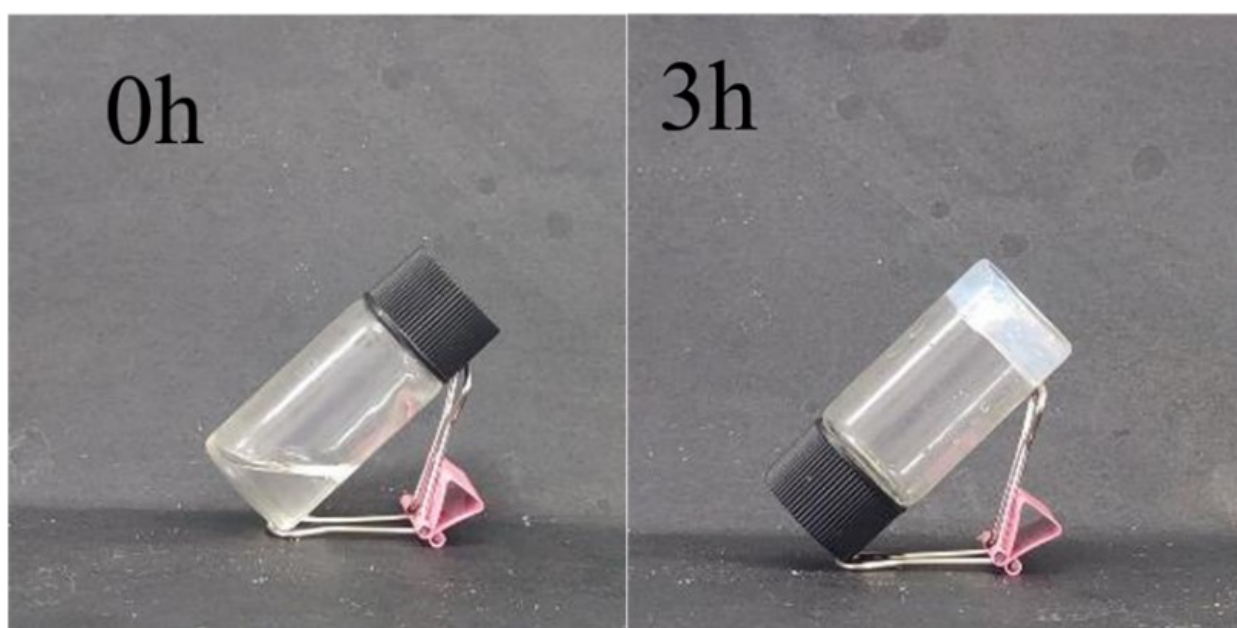
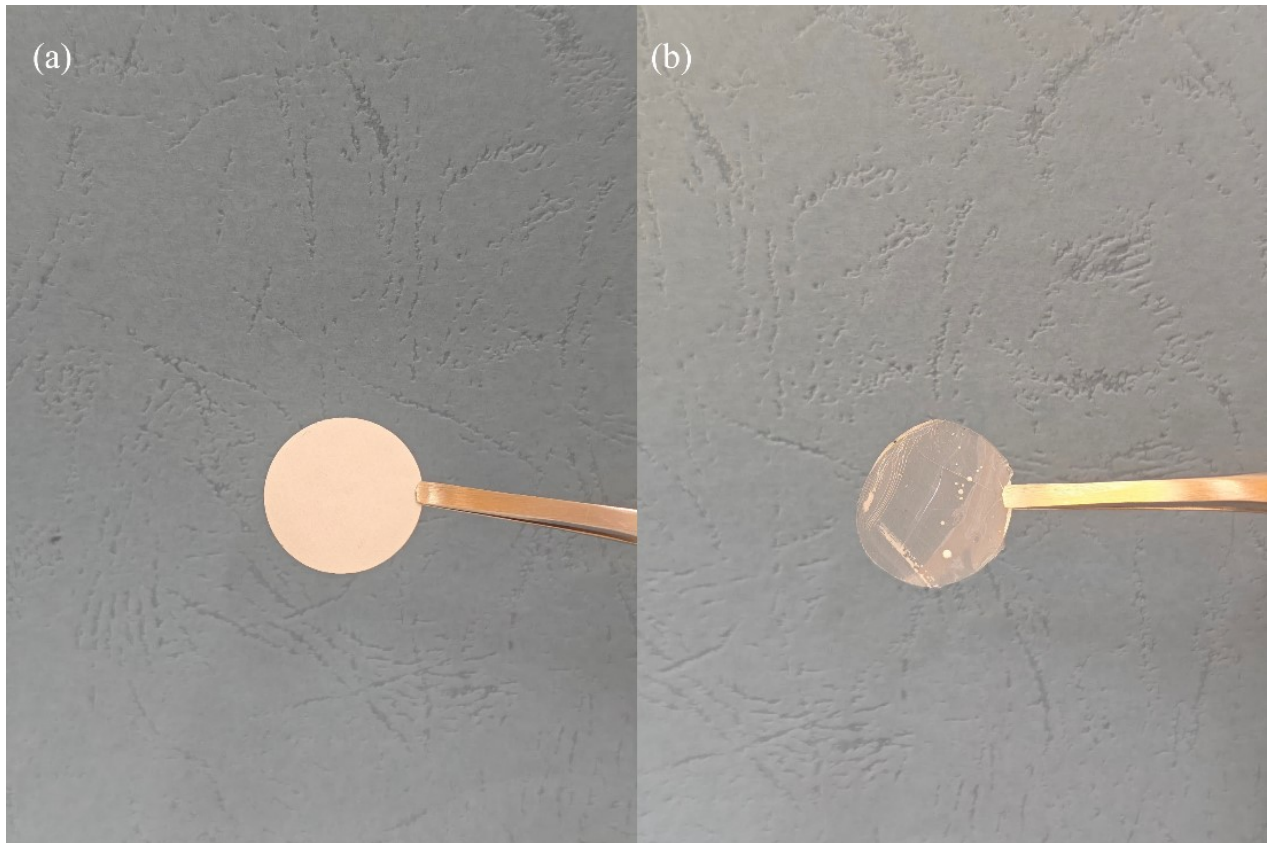


Fig. S1 (a)  $^1\text{H}$  NMR and (b) FT-IR spectra of DABP.



**Fig. S2** Liquid-solid transition of TDP118 from 0 h to 3 h.



**Fig. S3** Optical images of original cellulose membrane (a) and TDP118 (b).

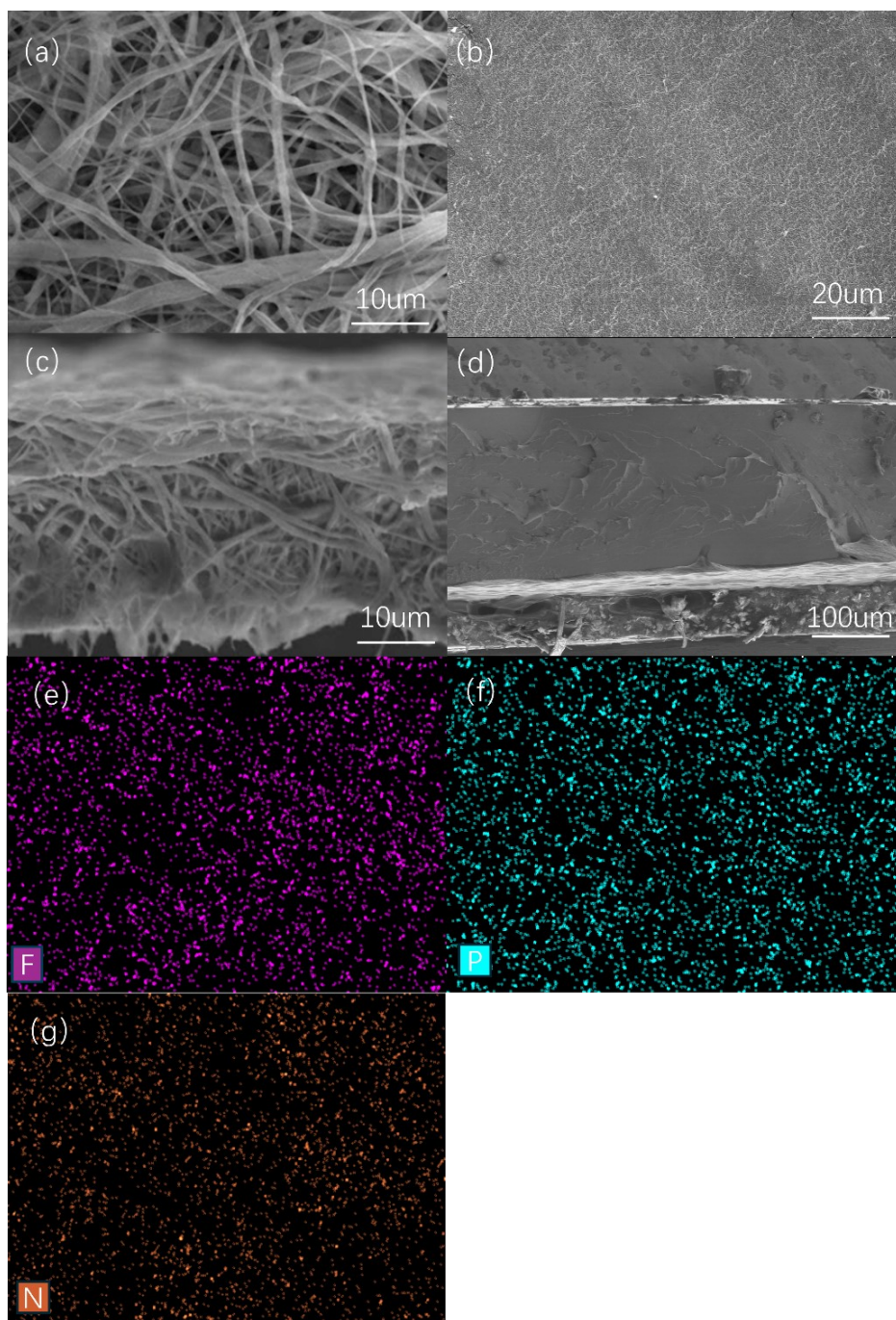


**Fig. S4** SEM images of (a) surface and (c) cross-section of the original cellulose membrane; (b) surface, (d) cross-section and (e-g) EDS mapping of TDP118.

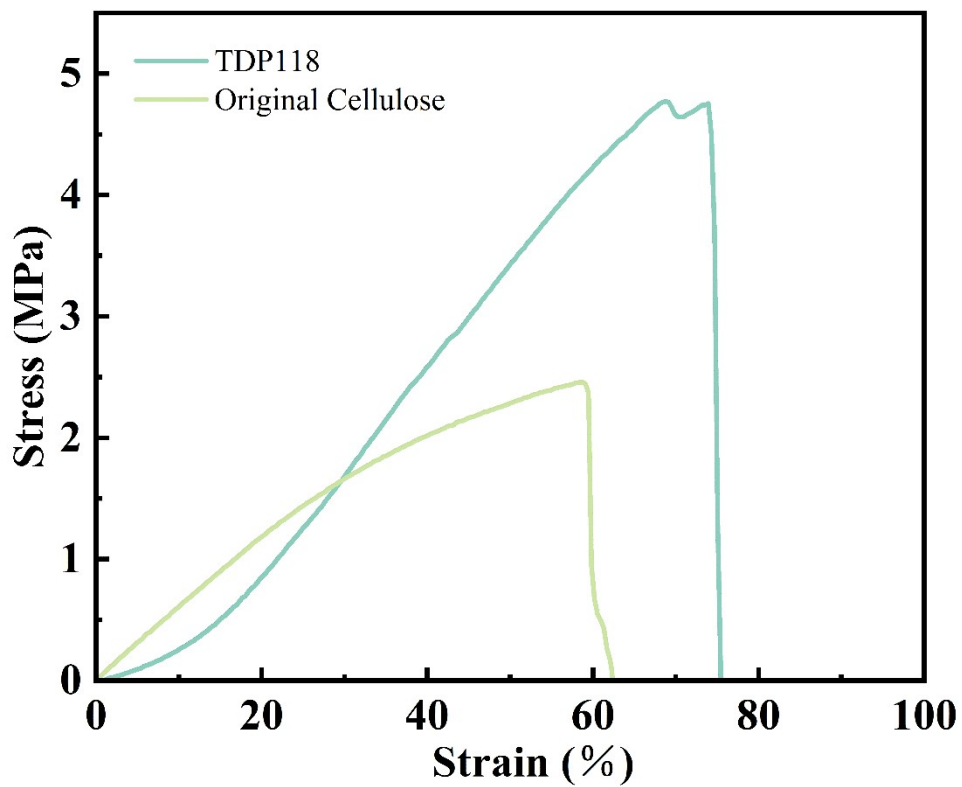


Fig. S5 Stress-strain curves of original cellulose membrane and TDP118.

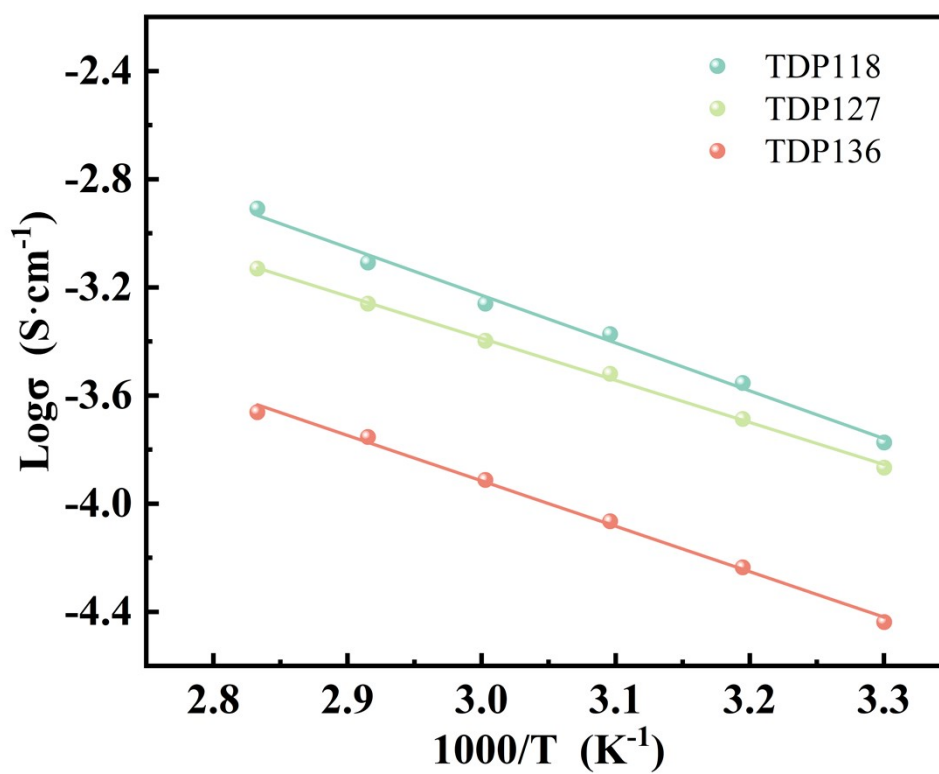


Fig. S6 The dependence of ionic conductivity on polymer compositions.

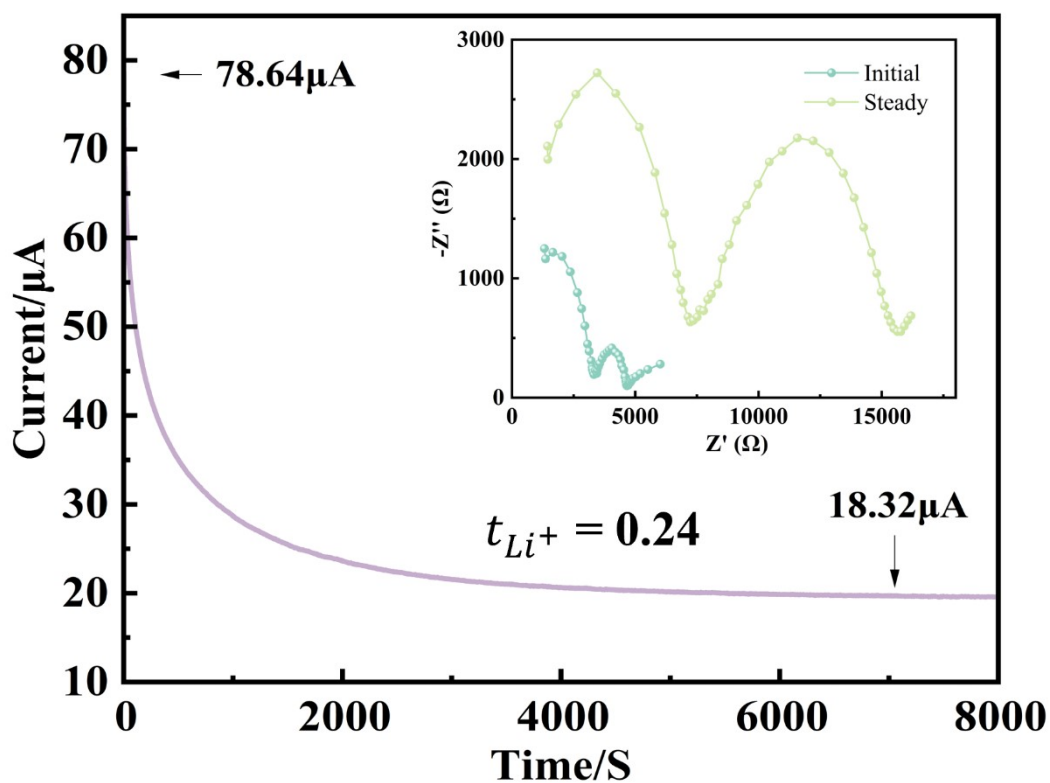


Fig.S7 Polarization curves obtained by chronoamperometry: inset shows the Nyquist plots of the symmetrical cell in the initial and steady states of PPEGMA.

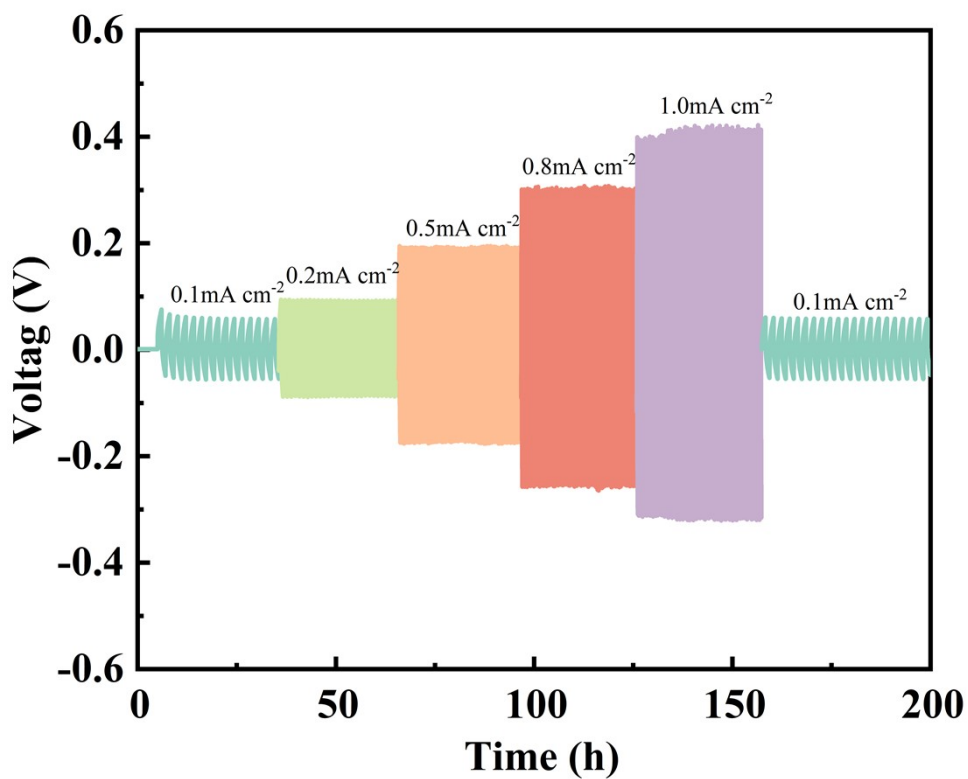
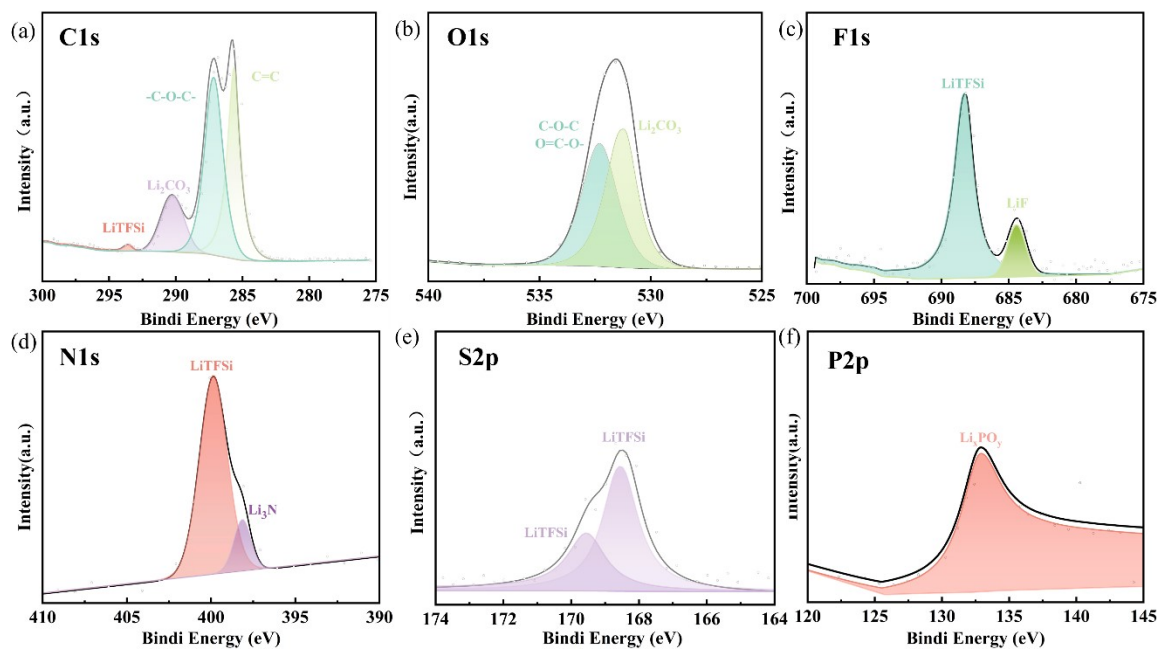


Fig. S8 The critical current density test of TDP118.



**Fig. S9** XPS analysis of the binding energy spectra of Li anodes in Li|TDP118|Li.

**Table S1** Room temperature ionic conductivity of TDP118 at different lithium salt concentrations.

Li salt content (wt.%)	10	15	20	25	30
Ionic Conductivity ( $S \cdot cm^{-1}$ )	$5.33 \times 10^{-5}$	$1.01 \times 10^{-4}$	$2.25 \times 10^{-4}$	$1.78 \times 10^{-4}$	$1.23 \times 10^{-4}$